PROCEEDINGS OF SPIE

SPIEDigitalLibrary.org/conference-proceedings-of-spie

Ultrasonic field mapping through a multimode optical fibre

Benjamin Keenlyside, Dylan Marques, Nathaniel Redgewell, Maxim Cherkashin, David Phillips, et al.

Benjamin Keenlyside, Dylan Marques, Nathaniel Redgewell, Maxim Cherkashin, David Phillips, Edward Zhang, Paul Beard, James Guggenheim, "Ultrasonic field mapping through a multimode optical fibre," Proc. SPIE 12631, Opto-Acoustic Methods and Applications in Biophotonics VI, 126310S (11 August 2023); doi: 10.1117/12.2675616

SPIE.

Event: European Conferences on Biomedical Optics, 2023, Munich, Germany

Downloaded From: https://www.spiedigitallibrary.org/conference-proceedings-of-spie on 19 Oct 2023 Terms of Use: https://www.spiedigitallibrary.org/terms-of-use

Ultrasonic field mapping through a multimode optical fibre

Benjamin Keenlyside[a], Dylan Marques[b,c,a], Nathaniel Redgewell[a], Maxim Cherkashin[a], David Phillips[d], Edward Zhang[a], Paul Beard[a], James Guggenheim[b,c,a]

[a]Department of Medical Physics and Biomedical Engineering, University College London, UK;
[b]Institute of Cardiovascular Sciences, University of Birmingham, Birmingham, UK;
[c]School of Engineering, University of Birmingham, Birmingham, UK;
[d]Department of Physics and Astronomy, University of Exeter, Exeter, UK.;

ABSTRACT

Miniaturising ultrasonic field mapping systems could lead to novel endoscopes capable of photoacoustic tomography and other techniques. However, developing high-resolution arrays of sensitive, sub-millimetre scale ultrasound sensors presents a challenge for traditional piezoelectric transducers. To address this challenge, we conceived an ultrasonic detection concept in which an optical ultrasonic sensor array is read out using a laser beam scanned through a 0.24 mm diameter multimode optical fibre using optical wavefront shaping. We demonstrate this system enables ultrasonic field mapping with >2500 measurement points, paving the way to developing miniaturised photoacoustic endoscopes and other ultrasonic systems based on the presented concept.

Keywords: Ultrasound, Wavefront shaping, Endoscope, Multimode Fibre

1. INTRODUCTION

Photoacoustic tomography (PAT) is an emerging biomedical imaging modality in which tissue is illuminated by laser pulses, and the resulting laser-generated ultrasound recorded using an ultrasound detector array[1]. The detected ultrasound waves are then used to digitally reconstruct a 3D image of specific absorbing structures (e.g. vasculature via hemoglobin absorption) in the tissue. There is a growing body of pre-clinical and clinical imaging applications using transcutaneous PAT systems[2], but extending PAT to an endoscopic regime could enable a range of new applications. These include surgical guidance, the early detection of cancers in the GI tract, and volumetric imaging in hard-to-reach sites in the body. However, developing endoscopic PAT systems using traditional methods is challenging, due to the difficulty in miniaturising piezoelectric transducer arrays.

One way of addressing this challenge is using all-optical Fabry-Perot (FP) ultrasound sensors[3]. These sensors comprise an optically clear layer between two mirrors, across which a laser beam is scanned in small steps to detect ultrasonic waves at an array of positions. Ultrasonically induced changes in the thickness of the sensor are detected interferometrically by monitoring the reflected power at a 'bias' wavelength close to the optical cavity resonance wavelength. This provides an ultrasonic array with an element size and pitch in the tens of microns, whose lateral dimensions can be scaled down to mm or even sub mm dimensions. This scalability makes PAT endoscopes based on the FP sensor an attractive proposition. However, a major challenge is finding a way to scan the interrogation laser across the sensor without needing a bulky optical scanner inside the endoscope. One solution is using an optical fibre bundle to deliver the beam to the sensor via fixed and spatially distinct channels[4]. This approach has enabled producing a 3.2 mm diameter PAT endoscope. An alternative approach, taken in this work, is to interrogate the FP sensor through a multimode optical fibre (MMF). This approach is attractive due to the high mode density of MMFs, which support >1000 independent spatial measurement channels through fibres with diameters as low as 100 µm. MMF is additionally low-cost, light-weight, flexible and MRI-compatible[5].

However, MMF presents a new challenge. Light transmitted through MMF is scrambled due to modal dispersion and coupling, and so a beam focused onto the proximal facet of the fibre will in general emerge as a pseudo-random speckle pattern on the fibre's distal side. Wavefront shaping (WFS)[6], originally developed to focus light through scattering materials[7], provides a solution to this problem. Despite its complexity, light propagation through MMF is still linear and deterministic, so it is possible to determine the wavefront that, after propagation through the fibre, emerges as beam focused at a desired position. Using a phase or amplitude spatial light modulator, these wavefronts can be sequentially generated,

Opto-Acoustic Methods and Applications in Biophotonics VI, edited by Chulhong Kim, Jan Laufer, Vasilis Ntziachristos, Roger J. Zemp, Proc. of SPIE Vol. 12631, 126310S
© 2023 SPIE · 0277-786X · doi: 10.1117/12.2675616

Downloaded From: https://www.spiedigitallibrary.org/conference-proceedings-of-spie on 19 Oct 2023
Terms of Use: https://www.spiedigitallibrary.org/terms-of-use

and a beam scanned across the distal facet of the MMF. This approach has been applied to a number of imaging modalities, including wide field optical[8], fluorescence[9] and photoacoustic[10,11] microscopy, and 3D time-of-flight[12] imaging.

We previously demonstrated that it is possible to make spatially localised ultrasound measurements by interrogating a planar FP ultrasound sensor through MMF[13]. However, the number of measurements positions was low, limited by the need to sequentially calibrate the wavefront needed for each focus. In this work, we demonstrate that it is possible to scale this approach in order to perform ultrasonic field mapping across an array of >2500 positions, a pre-requisite for practical endoscopic PAT imaging.

2. METHODS

2.1 Experimental Setup

A schematic of the prototype system used to perform all-optical ultrasonic mapping through an MMF is shown in Figure 1. The beam from a wavelength-tunable interrogation laser is expanded and filtered to produce a circular uniformly illuminated region on a liquid crystal Spatial Light Modulator (SLM). An MMF is placed with its proximal facet in the demagnified Fourier plane of the SLM. In this configuration a focused beam can be directed to a particular position on the fibre facet by displaying a blazed grating with the corresponding period and orientation on the SLM. The fibre tip was slightly displaced perpendicular to the optic axis of the system in order to filter out the 0th order unmodulated light. On the distal side of the MMF, the emitted laser beam is split via a beam-splitter, and delivered to the FP sensor and a co-planar CCD camera. In this configuration, the camera effectively allows imaging the illumination pattern incident on the sensor. The reflected light from the sensor is directed onto a photodiode, which records the reflected power.

2.2 Wavefront Shaping Algorithm

The wavefronts needed to form a focus at any position within the illuminated region of the sensor were determined in parallel, using the 'Transmission Matrix' (TM)[14] approach. In short, as transmission through a multimode fibre is linear and deterministic, it is possible to express the relationship between the input field $\boldsymbol{E_I}$ and output field $\boldsymbol{E_O}$ in the form:

$$\boldsymbol{E_O} = \begin{bmatrix} E_{o_1} \\ \vdots \\ E_{o_M} \end{bmatrix} = \begin{bmatrix} t_{11} & \cdots & t_{1N} \\ \vdots & \ddots & \vdots \\ t_{M1} & \cdots & t_{MN} \end{bmatrix} \begin{bmatrix} E_{i_1} \\ \vdots \\ E_{i_N} \end{bmatrix} = \boldsymbol{T E_I} \quad (1)$$

where E_{o_M} is the Mth output mode in a chosen output basis, E_{i_N} the Nth input mode in a (potentially different) input basis, and t_{ab} is a complex valued element of the transmission matrix T, giving the relative phase and amplitude of E_{o_a} when E_{i_b} is coupled into the fibre. The choice of input and output basis is arbitrary. If the transmission matrix is known, it can

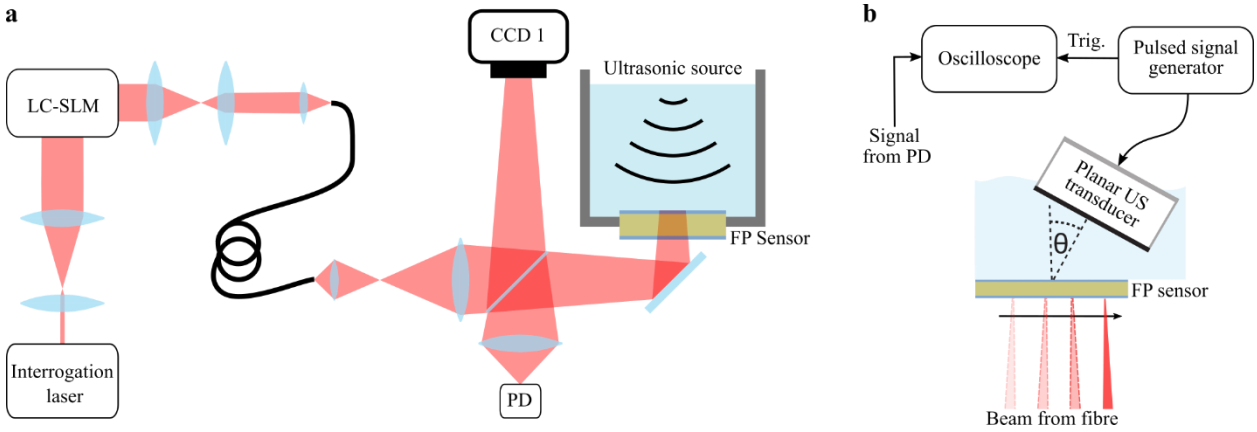

Figure 1 – (a) Schematic of the experimental system used to raster scan a focus across an FP sensor through MMF using WFS. The MMF used had an NA of 0.22 and a core diameter of 200µm, supporting approx. 2000 modes per polarisation. The magnified image of the fibre core on the sensor had a diameter of 5.4mm (b) Schematic of the experimental setup used in ultrasound field mapping experiments. The planar US transducer used had a centre frequency of 3.5MHz and a diameter of 22mm.

Downloaded From: https://www.spiedigitallibrary.org/conference-proceedings-of-spie on 19 Oct 2023
Terms of Use: https://www.spiedigitallibrary.org/terms-of-use

be used to straightforwardly find the conjugate input field $\boldsymbol{E_I}'$ needed to generate a desired output field $\boldsymbol{E_O}'$, as shown in Equation 2 (here we assume the TM is unitary so its inverse is equal to its conjugate transpose).

$$\boldsymbol{E_I}' = \boldsymbol{T}^{\dagger}\boldsymbol{E_O}' \tag{2}$$

In this work we measure the TM of the MMF by sequentially scanning a focused 'signal' beam across the proximal fibre tip using the SLM, and measuring the output field on a camera. In order to extract optical phase information from camera images the 'four-phase' method[15] was used, with a co-propagating internal reference. This involves generating a second focused 'reference' beam with the SLM, directed to a static position on the proximal fibre facet. For each signal beam position, the reference beam's phase was varied from 0 to 2π in four steps, and images recorded at each step. The phase and amplitude of the output field produced by the signal beam can be calculated from these images. Once the TM was measured, Equation 2 was used to calculate the sequence of phase patterns to display on the SLM in order to raster scan a focused beam on the distal side of the fibre.

2.3 Ultrasonic Measurements

When making ultrasonic (US) measurements, the configuration illustrated in Figure 1b. was used. A 22 mm diameter 3.5 MHz planar ultrasonic transducer, driven by a pulsed signal generator, was placed on the far side of the FP sensor. The transducer was placed at an angle to the sensor surface to produce a spatially varying US field. Acoustically-induced changes in reflected power detected by a photodiode in the path of the reflected light were recorded by an oscilloscope, triggered by the pulsed signal generator. In this way a time-resolved ultrasonic waveform could be recorded at any position that a WFS formed focus was directed toward. 2D field maps were produced by raster scanning the optical focus and making US measurements as described above at each position.

3. RESULTS

To investigate the quality of the foci produced by WFS using this system, a focus was scanned across a grid of 51x51 positions, regularly spaced by 160 μm in the plane of the sensor, and camera images recorded for each position. A Maximum Intensity Projection (MIP) through this set of images is shown in Figure 2a, with the boundaries of the fibre core and cladding marked. As expected, bright foci can be seen at a regular grid of positions within the fibre core. Weaker foci are also visible within the fibre cladding.

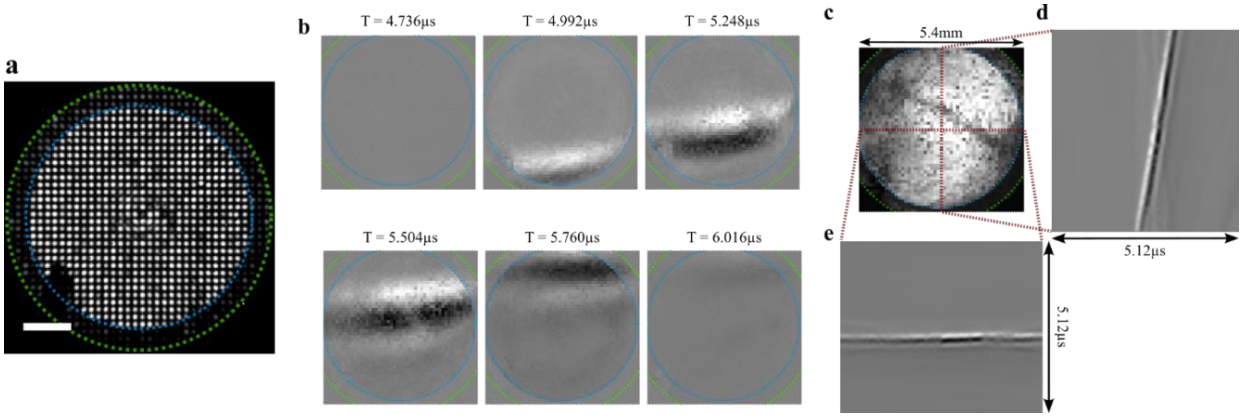

Figure 2 – (a) Maximum intensity projection (MIP) of a sequence of images of WFS-formed foci scanned over a regular array of target positions on an FP sensor. The scale bar corresponds to 1mm in the plane of the sensor (40μm on the distal fibre facet). The dashed rings indicate the boundary of the fibre core and cladding. (b) Snapshots of the recorded US pressure at 6 discrete time steps, showing the propagation of the US pulse across the FP sensor. (c) MIP of the full 2D ultrasound field scan. (d-e) US time-series cross sections across a pair of orthogonal axis. Both cross sections are through the centre of the mapped region, indicated by the respective dashed lines. All images (optical and acoustic) are plotted on a linear scale.

Downloaded From: https://www.spiedigitallibrary.org/conference-proceedings-of-spie on 19 Oct 2023
Terms of Use: https://www.spiedigitallibrary.org/terms-of-use

Focusing via WFS was possible at (nearly) any position within the fibre core, and through the fibre cladding at lower efficiency. The achieved peak-background intensity ratio (PBR) varied with focus position. Foci with a PBR of >1700 are produced at >97% of positions within the fibre core, with the maximum achieved PBR>3000.

An experiment was carried out to demonstrate US field mapping, using the known US field produced using the configuration shown in Figure 1b as a test field. US time series were recorded using the same array of foci positions shown in Figure 2a, building up a 2D field map.

A sequence of US pressure snapshots are shown in Figure 2b, taken from 6 different time-points in the full recorded ultrasound field. As expected, a tripolar US pulse is visible, travelling across the sensor with time, demonstrating the capability of this system to map US fields. An MIP of the full field map is shown in Figure 2c, to illustrate variations in measurement sensitivity. The boundaries between the fibre core and cladding are visible as a drop in the magnitude of the measured US signal. As the US transducer used is substantially larger than the mapped region, the true peak pressure can be assumed to be nearly constant across this area, and variation in the maximum recorded intensity acts as a proxy for measurement sensitivity. The difference in sensitivity between the core/cladding region is due to the aforementioned difference in WFS efficiency between these regions.

Cross-sections through the recorded ultrasound field are plotted in Figure 4d-e, showing the US time series for the points along the two marked lines, perpendicular to one another and meeting in the centre of the mapped US field region. As expected, the tripolar US pulse is visible in both cross sections, angled across one axis and nearly normally incident to the other. A weak signal is also seen in a band between the earliest and latest times of arrival of the US pulse. This is caused by background light that remains outside the WFS-formed focus, effectively producing weak cross-talk between the measurement positions.

4. CONCLUSIONS

A method for interrogating a FP sensor through MMF has been presented, using WFS to generate and raster scan a focused optical beam through the fibre. By determining the wavefronts needed to form each of these foci in parallel using a TM measurement method, it was possible to perform US field mapping through the fibre within a reasonable time. By providing a means to map US fields over arrays with many points through MMF, this work could enable the development of small endoscopic US and PAT imaging systems that are MR compatible and well-suited to multi-modal imaging through a single optical fibre. Potential applications include surgical guidance, monitoring cancers of the GI tract, and intravascular imaging at hard-to-reach sites in the body.

AKNOWLEDGEMENTS

This work is supported by: the EPSRC-funded Centre for Doctoral Training in Integrated Photonic and Electronic Systems (IPES) (EP/L015455/1); The Royal Society (URF\R1\180435, RGF\EA\181025); EPSRC (EP/S01800X/); ERC (Advanced Grant 74119) and The Welcome Trust/EPSRC (NS/A000050/1).

REFERENCES

[1] Beard, P., “Biomedical photoacoustic imaging,” Interface Focus **1**(4), 602–631 (2011).
[2] Li, L. and Wang, L. V., “Recent Advances in Photoacoustic Tomography,” BME Front **2021** (2021).
[3] Zhang, E., Laufer, J. and Beard, P., “Backward-mode multiwavelength photoacoustic scanner using a planar Fabry-Perot polymer film ultrasound sensor for high-resolution three-dimensional imaging of biological tissues,” Appl Opt **47**(4), 561–577 (2008).
[4] Ansari, R., Zhang, E. Z., Desjardins, A. E. and Beard, P. C., “All-optical forward-viewing photoacoustic probe for high-resolution 3D endoscopy,” Light Sci Appl **7**(1), 2047–7538 (2018).
[5] Taffoni, F., Formica, D., Saccomandi, P., Di Pino, G. and Schena, E., “Optical Fiber-Based MR-Compatible Sensors for Medical Applications: An Overview,” Sensors 2013, Vol. 13, Pages 14105-14120 **13**(10), 14105–14120 (2013).
[6] Vellekoop, I. M., “Feedback-based wavefront shaping,” Opt Express **23**(9), 12189 (2015).
[7] Vellekoop, I. M. and Mosk, A. P., “Focusing coherent light through opaque strongly scattering media,” Opt Lett **32**(16), 2309 (2007).

Downloaded From: https://www.spiedigitallibrary.org/conference-proceedings-of-spie on 19 Oct 2023
Terms of Use: https://www.spiedigitallibrary.org/terms-of-use

[8] Choi, Y., Yoon, C., Kim, M., Yang, T. D., Fang-Yen, C., Dasari, R. R., Lee, K. J. and Choi, W., "Scanner-free and wide-field endoscopic imaging by using a single multimode optical fiber," Phys Rev Lett **109**(20) (2012).

[9] Ohayon, S., Caravaca-Aguirre, A., Piestun, R. and DiCarlo, J. J., "Minimally invasive multimode optical fiber microendoscope for deep brain fluorescence imaging," Biomed Opt Express **9**(4), 1492 (2018).

[10] Zhao, T., Zhang, M., Ourselin, S. and Xia, W., "Wavefront Shaping-Assisted Forward-Viewing Photoacoustic Endomicroscopy Based on a Transparent Ultrasound Sensor," Applied Sciences 2022, Vol. 12, Page 12619 **12**(24), 12619 (2022).

[11] Mezil, S., Caravaca-Aguirre, A. M., Zhang, E. Z., Moreau, P., Wang, I., Beard, P. C. and Bossy, E., "Single-shot hybrid photoacoustic-fluorescent microendoscopy through a multimode fiber with wavefront shaping," Biomed Opt Express **11**(10), 5717 (2020).

[12] Stellinga, D., Phillips, D. B., Mekhail, S. P., Selyem, A., Turtaev, S., Čižmár, T. and Padgett, M. J., "Time-of-flight 3D imaging through multimode optical fibers," Science (1979) **374**(6573), 1395–1399 (2021).

[13] Keenlyside, B., Marques, D., Redgewell, N., Cherkashin, M., Zhang, E., Beard, P. and Guggenheim, J., "Spatially-resolved readout of a Fabry-Perot ultrasound sensor through a 125μm diameter optical fibre using wavefront shaping," in preparation (2023).

[14] Popoff, S. M., Lerosey, G., Carminati, R., Fink, M., Boccara, A. C. and Gigan, S., "Measuring the transmission matrix in optics: An approach to the study and control of light propagation in disordered media," Phys Rev Lett **104**(10) (2010).

[15] Dubois, A., Vabre, L., Boccara, A. C. and Beaurepaire, E., "High-resolution full-field optical coherence tomography with a Linnik microscope," Applied Optics, Vol. 41, Issue 4, pp. 805-812 **41**(4), 805–812 (2002).

Downloaded From: https://www.spiedigitallibrary.org/conference-proceedings-of-spie on 19 Oct 2023
Terms of Use: https://www.spiedigitallibrary.org/terms-of-use